

## 883 A Theory Parts

### 884 A.1 Proof of Theorem 3.1

885 The proof of Theorem 3.1 is based on the so-called Score-projection identity which was first found  
 886 in Vincent [60] to bridge denoising score matching and denoising auto-encoders. Later the identity  
 887 is applied by Zhou et al. [79] for deriving distillation methods based on Fisher divergences. We  
 888 appreciate the efforts of Zhou et al. [79] and re-write the score-projection identity here without proof.  
 889 Readers can check Zhou et al. [79] for a complete proof of score-projection identity.

890 **Theorem A.1.** Let  $\mathbf{u}(\cdot)$  be a vector-valued function, using the notations of Theorem 3.1, under mild  
 891 conditions, the identity holds:

$$\mathbb{E}_{\mathbf{x}_t \sim p_{\theta,t}} \mathbf{u}(\mathbf{x}_t)^T \left\{ \mathbf{s}_{p_{\theta,t}}(\mathbf{x}_t) - \nabla_{\mathbf{x}_t} \log q_t(\mathbf{x}_t | \mathbf{x}_0) \right\} = 0, \quad \forall \theta.$$

892 Next, we turn to prove the Theorem 3.1.

893 *Proof.* We prove a more general result. Let  $\mathbf{u}(\cdot)$  be a vector-valued function, the so-called score-  
 894 projection identity [79, 60] holds,

$$\mathbb{E}_{\mathbf{x}_t \sim p_{\theta,t}} \mathbf{u}(\mathbf{x}_t)^T \left\{ \mathbf{s}_{p_{\theta,t}}(\mathbf{x}_t) - \nabla_{\mathbf{x}_t} \log q_t(\mathbf{x}_t | \mathbf{x}_0) \right\} = 0, \quad \forall \theta. \quad (\text{A.1})$$

895 Notice that for most commonly used forward diffusion processes such as VP and VE process [57],  
 896 the term  $\nabla_{\mathbf{x}_t} \log q_t(\mathbf{x}_t | \mathbf{x}_0)$  turns out to be a scale of the difference of an added Gaussian noise  $\epsilon$ ,  
 897 therefore the  $\theta$  gradient for  $\nabla_{\mathbf{x}_t} \log q_t(\mathbf{x}_t | \mathbf{x}_0)$  will vanish. Taking  $\theta$  gradient on both sides of identity  
 898 (A.1), we have

$$0 = \mathbb{E}_{\mathbf{x}_t \sim p_{\theta,t}} \frac{\partial}{\partial \mathbf{x}_t} \left\{ \mathbf{u}(\mathbf{x}_t)^T \left\{ \mathbf{s}_{p_{\theta,t}}(\mathbf{x}_t) - \nabla_{\mathbf{x}_t} \log q_t(\mathbf{x}_t | \mathbf{x}_0) \right\} \right\} \frac{\partial \mathbf{x}_t}{\partial \theta} + \mathbb{E}_{\mathbf{x}_t \sim p_{\theta,t}} \mathbf{u}(\mathbf{x}_t)^T \frac{\partial}{\partial \theta} \left\{ \mathbf{s}_{p_{\theta,t}}(\mathbf{x}_t) \right\}$$

899 So we have an identity

$$\begin{aligned} \mathbb{E}_{\mathbf{x}_t \sim p_{\theta,t}} \mathbf{u}(\mathbf{x}_t)^T \frac{\partial}{\partial \theta} \left\{ \mathbf{s}_{p_{\theta,t}}(\mathbf{x}_t) \right\} &= -\mathbb{E}_{\mathbf{x}_t \sim p_{\theta,t}} \frac{\partial}{\partial \mathbf{x}_t} \left\{ \mathbf{u}(\mathbf{x}_t)^T \left\{ \mathbf{s}_{p_{\theta,t}}(\mathbf{x}_t) - \nabla_{\mathbf{x}_t} \log q_t(\mathbf{x}_t | \mathbf{x}_0) \right\} \right\} \frac{\partial \mathbf{x}_t}{\partial \theta} \\ &= -\frac{\partial}{\partial \theta} \mathbb{E}_{\mathbf{x}_t \sim p_{\theta,t}} \left\{ \mathbf{u}(\mathbf{x}_t) \left\{ \mathbf{s}_{p_{\text{sg}[\theta],t}}(\mathbf{x}_t) - \nabla_{\mathbf{x}_t} \log q_t(\mathbf{x}_t | \mathbf{x}_0) \right\} \right\} \end{aligned} \quad (\text{A.2})$$

900 Notice that the left-hand side of equation (A.2) can be interpreted as the gradient of the loss function  
 901 when the parameter dependency of the sampling distribution is cut off, i.e.

$$\mathbb{E}_{\mathbf{x}_t \sim p_{\theta,t}} \mathbf{u}(\mathbf{x}_t)^T \frac{\partial}{\partial \theta} \left\{ \mathbf{s}_{p_{\theta,t}}(\mathbf{x}_t) \right\} = \frac{\partial}{\partial \theta} \mathbb{E}_{\mathbf{x}_t \sim p_{\text{sg}[\theta],t}} \left\{ \mathbf{u}(\mathbf{x}_t)^T \mathbf{s}_{p_{\theta,t}}(\mathbf{x}_t) \right\} \quad (\text{A.3})$$

902 Therefore we have the final equation

$$\frac{\partial}{\partial \theta} \mathbb{E}_{\mathbf{x}_t \sim p_{\text{sg}[\theta],t}} \left\{ \mathbf{u}(\mathbf{x}_t)^T \mathbf{s}_{p_{\theta,t}}(\mathbf{x}_t) \right\} = -\frac{\partial}{\partial \theta} \mathbb{E}_{\mathbf{x}_t \sim p_{\theta,t}} \left\{ \mathbf{u}(\mathbf{x}_t) \left\{ \mathbf{s}_{p_{\text{sg}[\theta],t}}(\mathbf{x}_t) - \nabla_{\mathbf{x}_t} \log q_t(\mathbf{x}_t | \mathbf{x}_0) \right\} \right\} \quad (\text{A.4})$$

903 which holds for arbitrary function  $\mathbf{u}(\cdot)$  and parameter  $\theta$ . If we set

$$\begin{aligned} \mathbf{u}(\mathbf{x}_t) &= \mathbf{d}'(\mathbf{y}_t) \\ \mathbf{y}_t &= \mathbf{s}_{p_{\text{sg}[\theta],t}}(\mathbf{x}_t) - \mathbf{s}_{q_t}(\mathbf{x}_t) \end{aligned}$$

904 Then we formally have

$$\begin{aligned} &\frac{\partial}{\partial \theta} \mathbb{E}_{\mathbf{x}_t \sim p_{\text{sg}[\theta],t}} \left\{ \mathbf{d}'(\mathbf{y}_t) \right\}^T \left\{ \mathbf{s}_{p_{\theta,t}}(\mathbf{x}_t) \right\} \\ &= \frac{\partial}{\partial \theta} \mathbb{E}_{\substack{\mathbf{x}_0 \sim p_{\theta,0}, \\ \mathbf{x}_t | \mathbf{x}_0 \sim q_t(\mathbf{x}_t | \mathbf{x}_0)}} \left\{ -\mathbf{d}'(\mathbf{y}_t) \right\}^T \left\{ \mathbf{s}_{p_{\theta,t}}(\mathbf{x}_t) - \nabla_{\mathbf{x}_t} \log q_t(\mathbf{x}_t | \mathbf{x}_0) \right\} \end{aligned} \quad (\text{A.5})$$

905  $\square$

## 906 A.2 Pytorch style pseudo-code of Score Implicit Matching

907 In this section, we give a PyTorch style pseudo-code for algorithm 1, with the Pseudo-Huber distance  
 908 function. For a detailed algorithm on CIFAR10 with EDM model, please check Algorithm 2.

```

909 1 import torch
910 2 import torch.nn as nn
911 3 import torch.optim as optim
912 4
913 5 # Initialize generator G
914 6 G = Generator()
915 7
916 8 ## load teacher DM
917 9 Sd = DiffusionModel().load('/path_to_ckpt').eval().requires_grad_(False)
918 0 Sg = copy.deepcopy(Sd) ## initialize online DM with teacher DM
919 1
920 2 # Define optimizers
921 3 opt_G = optim.Adam(G.parameters(), lr=0.001, betas=(0.0, 0.999))
922 4 opt_Sg = optim.Adam(Sg.parameters(), lr=0.001, betas=(0.0, 0.999))
923 5
924 6 # Training loop
925 7 while True:
926 8     ## update Sg
927 9     Sg.train().requires_grad_(True)
928 0     G.eval().requires_grad_(False)
929 1
930 2     # loop for 2 times to update Sg
931 3     for _ in range(2):
932 4         z = torch.randn((2000, 2)).to(device)
933 5         with torch.no_grad():
934 6             fake_x = G(z)
935 7
936 8             t = torch.from_numpy(np.random.choice(np.arange(1, Sd.T), size=
937 fake_x.shape[0], replace=True)).to(device).long()
938 9             fake_xt, t, noise, sigma_t, g2_t = Sd(fake_x, t=t, return_t=True)
939 0             sigma_t = sigma_t.view(-1, 1).to(device)
940 1             g2_t = g2_t.to(device)
941 2             score = Sg(torch.cat([fake_xt, t.view(-1, 1)/Sd.T], -1))/sigma_t
942 3
943 4             batch_sg_loss = score + noise/sigma_t
944 5             batch_sg_loss = (g2_t*batch_sg_loss.square()).sum(-1).mean()*Sd.T
945 6
946 7             optimizer_Sg.zero_grad()
947 8             batch_sg_loss.backward()
948 9             optimizer_Sg.step()
949 0
950 1
951 2     ## update G
952 3     Sg.eval().requires_grad_(False)
953 4     G.train().requires_grad_(True)
954 5
955 6     z = torch.randn((2000, 2)).to(device)
956 7     fake_x = G(z)
957 8
958 9     t = torch.from_numpy(np.random.choice(np.arange(1, diffusion.T), size=
959 fake_x.shape[0], replace=True)).to(device).long()
960 0     fake_xt, t, noise, sigma_t, g2_t = diffusion(fake_x, t=t, return_t=
961 True)
962 1     sigma_t = sigma_t.view(-1, 1).to(device)
963 2     g2_t = g2_t.to(device)
964 3
965 4     score_true = Sd(torch.cat([fake_xt, t.view(-1, 1)/diffusion.T], -1))/
966 sigma_t
967 5     score_fake = Sg(torch.cat([fake_xt, t.view(-1, 1)/diffusion.T], -1))/
968 sigma_t

```

```

96866
97057 score_diff = score_true - score_fake
97158
97259 offset_coeff = denoise_diff / torch.sqrt(denoise_diff.square()).sum
973 ([1,2,3], keepdims=True) + self.phuber_c**2)
97460 weight = 1.0
97561
97662 batch_g_loss = weight * offset_coeff * (fake_denoise - images)
97763 batch_g_loss = batch_g_loss.sum([1,2,3]).mean()
97864
97965 optimizer_G.zero_grad()
98066 batch_g_loss.backward()
98167 optimizer_G.step()

```

Listing 1: Pytorch Style Pseudo-code of SIM

### 982 A.3 Instances of SIM with different distance functions

983 In section 3.3, we have discussed the powered normed as distance functions. Other choices, such as  
984 the Huber distance, which is defined as

$$\forall 1 \leq d \leq D, L_\delta(\mathbf{y})_d := \begin{cases} y_d^2/2 & \text{for } y_d \geq \delta \\ \delta(|y_d| - \delta/2) & \text{otherwise} \end{cases}$$

985 For other choices of distance functions, such as  $L1$  norm and exponential with powered norms, we  
986 put them in Table 4.

Table 4: Instances of Score Implicit Matching loss with different distance functions. The notations are aligned with the Algorithm 1.

CHOICE OF $\mathbf{d}(\cdot)$	$\mathbf{d}'(\mathbf{y}_t)$	LOSS FUNCTION
$\ \mathbf{y}_t\ _2^2$	$2\mathbf{y}_t$	$-2\mathbf{y}_t^T \left\{ \mathbf{s}_\psi(\mathbf{x}_t, t) - \nabla_{\mathbf{x}_t} \log q_t(\mathbf{x}_t \mathbf{x}_0) \right\}$
$\ \mathbf{y}_t\ _\alpha, \alpha \geq 1, \alpha \text{ even}$	$\alpha \mathbf{y}_t^{(\alpha-1)}$	$-\alpha \left\{ \mathbf{y}_t^{(\alpha-1)} \right\}^T \left\{ \mathbf{s}_\psi(\mathbf{x}_t, t) - \nabla_{\mathbf{x}_t} \log q_t(\mathbf{x}_t \mathbf{x}_0) \right\}$
$\exp(\beta \ \mathbf{y}_t\ _\alpha^\alpha) - 1, \alpha \geq 1, \alpha \text{ even}$	$\alpha \exp(\beta \ \mathbf{y}_t\ _\alpha^\alpha) \mathbf{y}_t^{(\alpha-1)}$	$-\alpha \exp(\beta \ \mathbf{y}_t\ _\alpha^\alpha) \left\{ \mathbf{y}_t^{(\alpha-1)} \right\} \left\{ \mathbf{s}_\psi(\mathbf{x}_t, t) - \nabla_{\mathbf{x}_t} \log q_t(\mathbf{x}_t \mathbf{x}_0) \right\}$
$\ \mathbf{y}_t\ _1$	$\text{sign}(\mathbf{y}_t)$	$-\text{sign}(\mathbf{y}_t)^T \left\{ \mathbf{s}_\psi(\mathbf{x}_t, t) - \nabla_{\mathbf{x}_t} \log q_t(\mathbf{x}_t \mathbf{x}_0) \right\}$
$L_\delta(\cdot)$ HUBER LOSS	$\frac{\partial}{\partial \mathbf{y}_t} L_\delta(\mathbf{y}_t)$	$-\frac{\partial}{\partial \mathbf{y}_t} L_\delta(\mathbf{y}_t)^T \left\{ \mathbf{s}_\psi(\mathbf{x}_t, t) - \nabla_{\mathbf{x}_t} \log q_t(\mathbf{x}_t \mathbf{x}_0) \right\}$
$\sqrt{\ \mathbf{y}_t\ _2^2 + c^2} - c$	$2 \frac{\mathbf{y}_t}{\sqrt{\ \mathbf{y}_t\ _2^2 + c^2}}$	$-2 \left\{ 2 \frac{\mathbf{y}_t}{\sqrt{\ \mathbf{y}_t\ _2^2 + c^2}} \right\}^T \left\{ \mathbf{s}_\psi(\mathbf{x}_t, t) - \nabla_{\mathbf{x}_t} \log q_t(\mathbf{x}_t \mathbf{x}_0) \right\}$

## 987 B Empirical Parts

### 988 B.1 Answer for the human preference study

989 The answer to the human preference study in Figure 1 is

- 990 • the middle image of the first row is generated by one-step SIM-DiT-600M;
- 991 • the leftmost image of the second row is generated by one step SIM-DiT-600M;
- 992 • the leftmost image of the third row is generated by one-step SIM-DiT-600M.

### 993 B.2 Experiment details on CIFAR10 dataset

994 We follow the experiment setting of SiD and DI on CIFAR10. We start with a brief introduction to  
995 the EDM model [21].

996 The EDM model depends on the diffusion process

$$d\mathbf{x}_t = t d\mathbf{w}_t, t \in [0, T]. \quad (\text{B.1})$$

997 Samples from the forward process (B.1) can be generated by adding random noise to the output of  
 998 the generator function, i.e.,  $\mathbf{x}_t = \mathbf{x}_0 + t\epsilon$  where  $\epsilon \sim \mathcal{N}(\mathbf{0}, \mathbf{I})$  is a Gaussian vector. The EDM model  
 999 also reformulates the diffusion model’s score matching objective as a denoising regression objective,  
 1000 which writes,

$$\mathcal{L}(\psi) = \int_{t=0}^T \lambda(t) \mathbb{E}_{\mathbf{x}_0 \sim p_0, \mathbf{x}_t | \mathbf{x}_0 \sim p_t(\mathbf{x}_t | \mathbf{x}_0)} \|\mathbf{d}_\psi(\mathbf{x}_t, t) - \mathbf{x}_0\|_2^2 dt. \quad (\text{B.2})$$

1001 Where  $\mathbf{d}_\psi(\cdot)$  is a denoiser network that tries to predict the clean sample by taking noisy samples  
 1002 as inputs. Minimizing the loss (B.2) leads to a trained denoiser, which has a simple relation to the  
 1003 marginal score functions as:

$$\mathbf{s}_\psi(\mathbf{x}_t, t) = \frac{\mathbf{d}_\psi(\mathbf{x}_t, t) - \mathbf{x}_t}{t^2} \quad (\text{B.3})$$

1004 Under such a formulation, we actually have pre-trained denoiser models for experiments. Therefore,  
 1005 we use the EDM notations in later parts.

1006 **Construction of the one-step generator.** Let  $\mathbf{d}_\theta(\cdot)$  be pretrained EDM denoiser models. Owing to  
 1007 the denoiser formulation of the EDM model, we construct the generator to have the same architecture  
 1008 as the pre-trained EDM denoiser with a pre-selected index  $t^*$ , which writes

$$\mathbf{x}_0 = g_\theta(\mathbf{z}) := \mathbf{d}(\mathbf{z}, t^*), \quad \mathbf{z} \sim \mathcal{N}(\mathbf{0}, (t^*)^2 \mathbf{I}). \quad (\text{B.4})$$

1009 We initialize the generator with the same parameter as the teacher EDM denoiser model.

1010 **Time index distribution.** When training both the EDM diffusion model and the generator, we need  
 1011 to randomly select a time  $t$  in order to approximate the integral of the loss function (B.2). The EDM  
 1012 model has a default choice of  $t$  distribution as log-normal when training the diffusion (denoiser)  
 1013 model, i.e.

$$t \sim p_{EDM}(t) : t = \exp(s) \quad (\text{B.5})$$

$$s \sim \mathcal{N}(P_{mean}, P_{std}^2), \quad P_{mean} = -1.2, P_{std} = 1.2. \quad (\text{B.6})$$

1014 And a weighting function

$$\lambda_{EDM}(t) = \frac{(t^2 + \sigma_{data}^2)}{(t \times \sigma_{data})^2}. \quad (\text{B.7})$$

1015 In our algorithm, we follow the same setting as the EDM model when updating the online diffusion  
 1016 (denoiser) model.

1017 In SiD, they propose to use a special discrete time distribution, which writes

$$\begin{aligned} \sigma_k &= (\sigma_{max}^\rho \frac{i}{K-1} (\sigma_{min}^\rho - \sigma_{max}^\rho))^\rho, \\ \sigma_{max} &= 80.0, \sigma_{min} = 0.002, \rho = 7.0, K = 1000 \end{aligned}$$

1018 They proposed to choose  $t$  uniformly from

$$t \sim p_{SiD}(t) : k \sim \text{Unif}[0, 800], t = \sigma_k; \quad (\text{B.8})$$

1019 We name such a time distribution the *Karr* distribution in Figure 2 because such a schedule was  
 1020 originally proposed in Karras’ EDM work for sampling.

1021 However, in practice, we find that *Karr* distribution (B.8) empirically does not work well. Instead,  
 1022 we find that a modified log-normal time distribution when updating the generation with SIM works  
 1023 better than *Karr* distribution. Our SIM time distribution writes:

$$t \sim p_{SIM}(t) : t = \exp(s) \quad (\text{B.9})$$

$$s \sim \mathcal{N}(P_{mean}, P_{std}^2), \quad P_{mean} = -3.5, P_{std} = 2.5. \quad (\text{B.10})$$

Table 5: Hyperparameters used for SIM on CIFAR10 EDM Distillation

Hyperparameter	CIFAR-10 (Uncond)		CIFAR-10 (Cond)	
	DM $s_\psi$	Generator $g_\theta$	DM $s_\psi$	Generator $g_\theta$
Learning rate	1e-5	1e-5	1e-5	1e-5
Batch size	256	256	256	256
$\sigma(t^*)$	2.5	2.5	2.5	2.5
Adam $\beta_0$	0.0	0.0	0.0	0.0
Adam $\beta_1$	0.999	0.999	0.999	0.999
Time Distribution	$p_{EDM}(t)$ (B.5)	$p_{SIM}(t)$ (B.9)	$p_{EDM}(t)$ (B.5)	$p_{SIM}(t)$ (B.9)
Weighting	$\lambda_{EDM}(t)$ (B.7)	1	$\lambda_{EDM}(t)$ (B.7)	1
Loss function	(B.2)	(??)	(B.2)	(B.2)
Number of GPUs	4×A100-40G	4×A100-40G	4×A100-40G	4×A100-40G

---

**Algorithm 2:** SIM with Pseudo-Huber distance for distilling EDM teacher [Pytorch Style].

---

**Input:** pre-trained EDM denoiser  $\mathbf{d}_{q_t}(\cdot)$ , generator  $g_\theta$ , prior distribution  $p_z$ , online EDM denoiser  $\mathbf{d}_\psi(\cdot)$ ; differentiable distance function  $\mathbf{d}(\cdot)$ , and forward diffusion (2.1).

**while not converge do**

    // freeze  $\theta$ , update  $\psi$ :

$\mathbf{x}_0 = g_\theta(\mathbf{z}).detach()$ ,  $\mathbf{z} \sim p_z$

$t \sim p_{EDM}(t)$ ,  $\mathbf{x}_t = \mathbf{x}_0 + t\epsilon$ ,  $\epsilon \sim \mathcal{N}(\mathbf{0}, \mathbf{I})$

$\mathcal{L}(\psi) = \lambda_{EDM}(t) \times \|\mathbf{d}_\psi(\mathbf{x}_t, t) - \mathbf{x}_0\|_2^2$

$\mathcal{L}(\psi).backward()$ ; update  $\psi$

    // freeze  $\psi$ , update  $\theta$ :

$\mathbf{x}_0 = g_\theta(\mathbf{z})$ ,  $\mathbf{z} \sim p_z$

$t \sim p_{SIM}(t)$ ,  $\mathbf{x}_t = \mathbf{x}_0 + t\epsilon$ ,  $\epsilon \sim \mathcal{N}(\mathbf{0}, \mathbf{I})$

$\mathcal{L}(\theta) = -\left\{ \frac{\mathbf{y}_t}{\sqrt{\|\mathbf{y}_t\|_2^2 + c^2}} \right\}^T \left\{ \mathbf{d}_\psi(\mathbf{x}_t, t) - \mathbf{x}_0 \right\}$ , where  $\mathbf{y}_t := \mathbf{d}_\psi(\mathbf{x}_t, t) - \mathbf{d}_{q_t}(\mathbf{x}_t)$

$\mathcal{L}(\theta).backward()$ ; update  $\theta$

**end**

**return**  $\theta, \psi$ .

---

1024 **Weighting function.** As we have said, we use the same  $\lambda_{EDM}(t)$  (B.7) weighting function as  
1025 EDM when updating the denoiser model. When updating the generator, SiD uses a specially designed  
1026 weighting function, which writes:

$$w_{SiD}(t) = \frac{C \times t^4}{\|\mathbf{x}_0 - \mathbf{d}_{q_t}(\mathbf{x}_t)\|_{1,sg}} \quad (\text{B.11})$$

$$\mathbf{x}_t = \mathbf{x}_0 + t\epsilon, \quad \epsilon \sim \mathcal{N}(\mathbf{0}, \mathbf{I}) \quad (\text{B.12})$$

1027 The notation sg means stop-gradient, and  $C$  is the data dimensions. They claim such a weighting  
1028 function helps to stabilize the training. However, in our experiments, since the SIM itself has  
1029 normalized the loss (see section 4), we do not use such ad-hoc weighting functions. Instead, we just  
1030 set the weighting function to be 1 for all time. We call the SiD’s weighting function the *sidwgt* in  
1031 Figure 2, and our weighting the *nowgt* in Figure 2.

1032 In Figure 2, we compare the SiD and SIM with different time distribution and weighting functions.  
1033 We find that SIM+nowgt+lognormal time distribution gives the best performances significantly,  
1034 therefore our final experiment tasks such a configuration. Table 5 records the detailed configurations  
1035 we use for SIM on CIFAR10 EDM distillation.

1036 With the optimal setting and EDM formulation, we can rewrite our algorithm in an EDM style in  
1037 Algorithm 2.

### 1038 B.3 Experiment details on Text-to-Image Distillation

1039 In the Text-to-Image distillation part, in order to align our experiment with that on CIFAR10, we  
1040 rewrite the PixArt- $\alpha$  model in EDM formulation:

$$D_\theta(\mathbf{x}; \sigma) = \mathbf{x} - \sigma F_\theta \quad (\text{B.13})$$

1041 Here, following the iDDPM+DDIM preconditioning in EDM, PixArt- $\alpha$  is denoted by  $F_\theta$ ,  $\mathbf{x}$  is the  
 1042 image data plus noise with a standard deviation of  $\sigma$ , for the remaining parameters such as  $C_1$  and  
 1043  $C_2$ , we kept the other parameters unchanged to match those defined in EDM. Unlike the original  
 1044 model, we only retained the image channels for the output of this model. Since we employed the  
 1045 preconditioning of iDDPM+DDIM in the EDM, each  $\sigma$  value is rounded to the nearest 1000 bins  
 1046 after being passed into the model. For the actual values used in PixArt- $\alpha$ , beta\_start is set to 0.0001,  
 1047 and beta\_end is set to 0.02. Therefore, according to the formulation of EDM, the range of our noise  
 1048 distribution is [0.01, 156.6155], which will be used to truncate our sampled  $\sigma$ . For our one-step  
 1049 generator, it is formulated as:

$$g_\theta(\mathbf{x}; \sigma_{\text{init}}) = \mathbf{x} - \sigma_{\text{init}} F_\theta \quad (\text{B.14})$$

1050 Here following SiD  $\sigma_{\text{init}} = 2.5$  and  $\mathbf{x} \sim \mathcal{N}(0, \sigma_{\text{init}} \mathbf{I})$ , we observed in practice that larger values of  
 1051  $\sigma_{\text{init}}$  lead to faster convergence of the model, but the difference in convergence speed is negligible for  
 1052 the complete model training process and has minimal impact on the final results.

1053 We utilized the SAM-LLaVA-Caption10M dataset, which comprises prompts generated by the LLaVA  
 1054 model on the SAM dataset. These prompts provide detailed descriptions for the images, thereby  
 1055 offering us a challenging set of samples for our distillation experiments.

1056 All experiments in this section were conducted on 4 A100-40G GPUs with bfloat16 precision, using  
 1057 the PixArt-XL-2-512x512 model version, employing the same hyperparameters. For both optimizers,  
 1058 we utilized Adam with a learning rate of 5e-6 and betas=[0, 0.999]. Additionally, to enable a batch  
 1059 size of 1024, we employed gradient checkpointing and set the gradient accumulation to 8. Finally,  
 1060 regarding the training noise distribution, instead of adhering to the original iDDPM schedule, we  
 1061 sample the  $\sigma$  from a log-normal distribution with a mean of -2.0 and a standard deviation of 2.0, we  
 1062 use the same noise distribution for both optimization step and set the two loss weighting to constant  
 1063 1. Our best model was trained on the SAM Caption dataset for approximately 16k iterations, which is  
 1064 equivalent to less than 2 epochs. This training process took about 2 days on 4 A100-40G GPUs.

1065 We also tested the impact of different noise distributions on the distillation process. When the noise  
 1066 distribution is highly concentrated around smaller values, we observed a phenomenon where the  
 1067 generated samples appear excessively dark. On the other hand, when we used slightly larger noise  
 1068 distributions, we found that the structure of the generated samples tended to be unstable.

#### 1069 B.4 Instruction for Human Preference Study

1070 Our user study primarily focuses on comparing the outputs of the distilled model and the teacher  
 1071 model. Each image has undergone rigorous manual review to ensure the safety of survey participants.  
 1072 We conducted the study using questionnaires, where users were presented with two randomly ordered  
 1073 images generated by the distilled model and teacher model and asked to select the sample that best  
 1074 matched the text description and had higher image quality. Finally, we used the collected votes for  
 1075 the distilled model and the teacher model as indicators of user preference. The questionnaire website  
 1076 used for conducting these evaluations are shown in Figure 4.

1077 To be more specific, we randomly selected 17 prompt words and generated images of resolution  
 1078 512x512 using both the student model and the teacher model. To facilitate comparison, we presented  
 1079 the two images side by side in random order. In the questionnaire, we provided the complete prompt  
 1080 words for reference in addition to the generated images. In the end, we collected approximately 30  
 1081 survey responses in total.

#### 1082 B.5 Generated Samples on CIFAR10

#### 1083 B.6 Prompts for Figure 3

- 1084 • prompt for first row of Figure 3: *A small cactus with a happy face in the Sahara desert.*
- 1085 • prompt for second row of Figure 3: *An image of a jade green and gold coloured Fabergé*  
 1086 *egg, 16k resolution, highly detailed, product photography, trending on artstation, sharp*  
 1087 *focus, studio photo, intricate details, fairly dark background, perfect lighting, perfect com-*  
 1088 *position, sharp features, Miki Asai Macro photography, close-up, hyper detailed, trending*  
 1089 *on artstation, sharp focus, studio photo, intricate details, highly detailed, by greg rutkowski.*
- 1090 • prompt for third row of Figure 3: *Baby playing with toys in the snow.*

**AIGC Text-to-Image User Study**

B I U ↺ ↻

Given the following prompts, select the best image by text similarity and image quality. (17 text-image pairs in total)

1. Given the following prompts, select the best image by text similarity and image quality. \*  
"A small cactus with a happy face in the Sahara desert."



left  
 right

Figure 4: Demonstration of our human preference user study interface.



Figure 5: One-step SIM model on CIFAR10-conditional. FID=1.96.

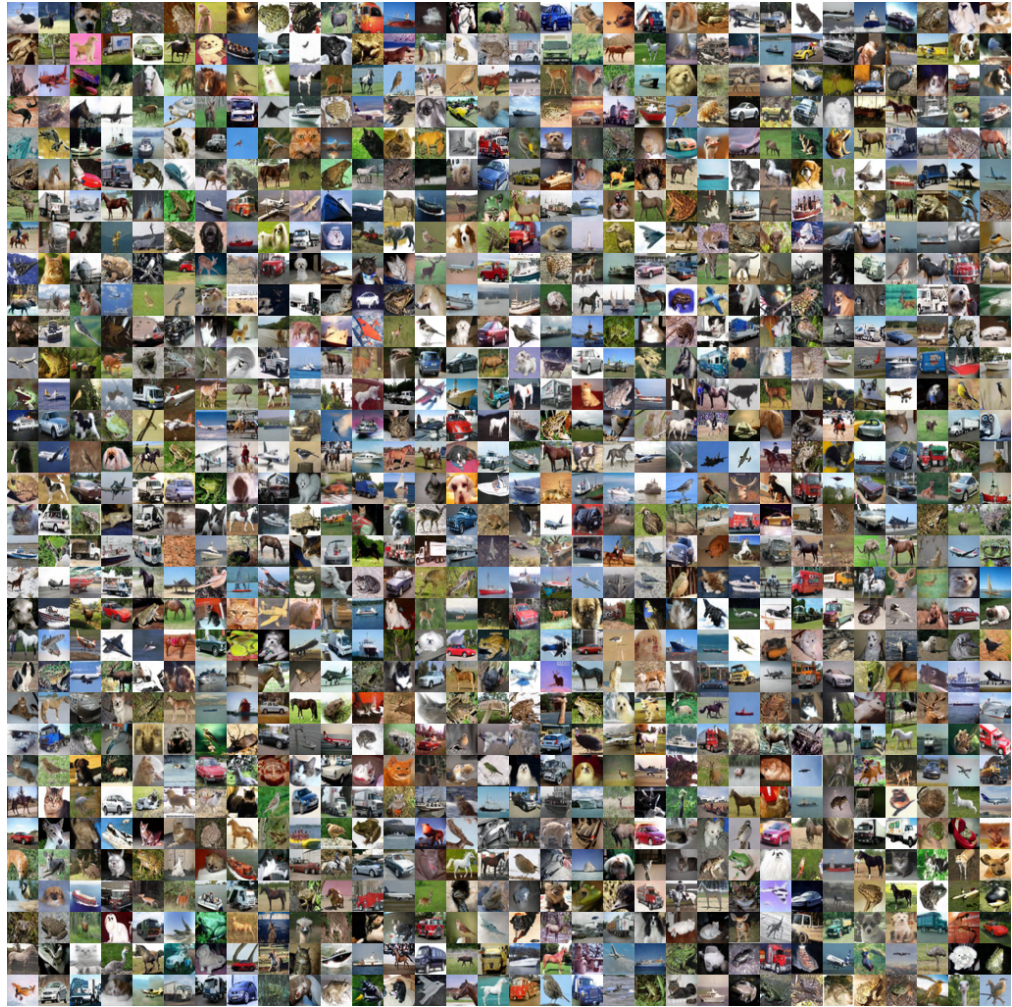


Figure 6: One-step SIM model on CIFAR10-unconditional. FID=2.17.